Performance of a Silica-polyethyleneimine Adsorbent for Post-Combustion CO_2 Capture on a 100 Kg Scale in a Fluidized Bed Continuous Unit

Jae-Young Kim[a], Je-Min Woo[a], Sung-Ho Jo[a], Hyunuk Kim[a], Seung-Yong Lee[a], Chang-Keun Yi[a], Jong-Ho Moon[a,b], Hyungseok Nam[a], Yooseob Won[a], Lee A. Stevens[c], Chenggong Sun[c], Hao Liu[c], Jingjing Liu[c], Colin E. Snape[c†] and Young Cheol Park[a†]

[a]*Korea Institute of Energy Research, 152 Gajeong-ro, Yuseong-gu, Daejeon 34129, Republic of Korea*

[b]*Chungbuk National University, 1 Chungdae-ro, Seowon-gu, Chungbuk Cheongju 28644, Republic of Korea*

[c]*University of Nottingham, Faculty of Engineering, The Energy Technologies Building, Triumph Road, Nottingham, NG7 2Tu, UK*

[†]Corresponding author.

Y.C. Park (youngchp@kier.re.kr), C.E. Snape (Colin.Snape@nottingham.ac.uk)

Highlight

- Silica-PEI adsorbent has been evaluated on a 100 kg scale in 150 h continuous test
- Optimal gas velocity for adsorbent in a bubbling fluidized-bed reactor was 5.1 cm/s
- ≥905% CO_2 removal efficiency with ≥7.5% dynamic sorption capacity achieved
- Working capacity decreased with an increase of CO_2 partial pressure in desorber
- CO_2 sorption performance of the adsorbents decreased as testing time increased

Abstract

Although basic silica-polyethyleneimine (PEI) adsorbents have received considerable attention as leading candidates for post-combustion capture, including use in a small number of pilot-scale studies, no detailed performance evaluation under specific conditions has been reported. In this study, a fluidized bed continuous unit has been used over a 150 h period to test the performance of a 100 kg sample of silica-PEI, containing 40 wt.% of PEI with a molecular mass of 5000, which was found to offer the best compromise between performance and ease of preparation, which ~~. The manufacture~~ involved minimizing the amount of water used ~~and using a commercial double cone vacuum dryer~~. The CO_2 removal efficiency and dynamic sorption capacity has been evaluated continuously ~~in a continuous way by~~ changing a number of variables. For the sorption reactor, the variables were inlet H_2O concentrations of 0–8.3 vol.%, inlet CO_2 concentrations of 12.2–20.5 vol.%, bed temperatures of 50–69ºC and the bed differential pressures of 176–3576~~8~~ mmH_2O have been changed. For the desorption reactor operated at the bed temperature of 130ºC, inlet H_2O concentrations of 8.2–13.6 vol.%, inlet CO_2 concentrations of 14.6–81.2 vol.% and ~~the~~ bed differential pressures of 4753~~4~~–580 mmH_2O were used~~varied~~. During continuous operation, ~~the~~CO_2 removal efficiencies of over 90% with dynamic sorption capacities of 7.5 wt.% were achieved.

~~maximum CO_2 removal efficiency achieved was 98.6% with a 6.3 wt.% dynamic sorption capacity~~. Each sample collected after adsorption and desorption during continuous operation were analyzed by TGA and ^{13}C-NMR to identity the decrease of equilibrium adsorption capacity and the extent of thermo-oxidative side reactions. Slow oxidative degradation of the silica-PEI occurred because of the non-humidified air in the transport the adsorbent between the two bubbling beds and, for some of the time, in the sorption reactor.

Keywords: Post-combustion CO_2 capture, Silica-PEI adsorbent, 100 kg scale fluidized bed continuous unit, CO_2 purity, Oxidative degradation.

1. Introduction

Post combustion CO_2 capture using solid sorbents is one of the most promising technologies, which can be classified as a second or third generation capture technology. Even though potential breakthrough materials have been recently developed, such materials still require the right material selection, proper sorbent characterization, and equilibrium testing over extended periods. Additionally, the commercialization of the technology needs further developments on sorbent materials which can be used under real flue gas conditions with various actual conditions including impurities, checking dynamic loading, stability and lifetime in continuous operation. There have only been a few reported studies applying solid sorbents in continuous operation in systems similar to the actual process. Potassium carbonate (K)-based solid sorbents have been applied in a continuous operation in a bench-scale [1–3], a 0.5 MWe test-bed [4], and a 10 MWe pilot-scale [5,6] process. Amine-based solid sorbents have been applied in a continuous operation in a laboratory-scale [7], bench-scale [8], 1 MWe pilot-scale [9–11].

Compared with K-based solid sorbents, amine-based ones have been known to be promising as they can reduce the regeneration energy because of its lower heat of adsorption and high dynamic sorption capacity. Among amine-based sorbents, silica-polyethyleneimine (PEI) has been widely developed by Sayari and coworkers [12–18], Jones and coworkers [19–25], Choi and coworkers [26–31] and Snape and coworkers [32–36]. Sayari and coworkers [16–18] and Jones and coworkers [22–25] reported the largest single body of work on the application of amine-grafted silica materials for CO_2 adsorption. Choi and coworkers hypothesized that the high propensity of PEI to oxidative degradation may be associated with the occurrence of transition metal impurities within the polymer. They not only confirmed the presence of such trace metals in the polymer, but they were able to inhibit its oxidative degradation to a great

extent by adding chelating agents to sequester such cations [29,30]. Snape and coworkers have investigated mesoporous silica impregnating a mass fraction of 40 wt.% PEI into a commercial mesoporous silica support [32–36]. They evaluated the sorption performance of silica-PEI adsorbent under different working conditions (w/ and w/o the presence of moisture, different gas-solid contact times, initial bed temperatures and CO_2 partial pressures) using a laboratory-scale bubbling fluidized bed reactor [34]. The working capacity of the silica-PEI adsorbent was one of the most important parameters affecting the sorbent regeneration heat energy. The operating conditions investigated were physical properties of adsorbent, the heat of adsorption, specific heat capacity, working capacity, moisture adsorption of the silica-PEI adsorbent, the swing temperature difference and the degree of heat recovery [35].

KIER has developed a dry CO_2 capture process using solid sorbents [37–44], and the research results on CO_2 capture have been steadily reported in a laboratory-scale, a bench-scale, a pilot-scale process [1,2,4–6,45,46]. Recently, Kim et al. evaluated the CO_2 capture performance of silica-PEI adsorbent in a lab.-scale TBS (twin bubbling fluidized-bed system) where 24 h preliminary tests were performed using 5 kg of adsorbent where the PEI with a molecular mass of 800. A 180-hour continuous test was then conducted using PEI with a molecular mass of 5000 (S.PEI-5K) to investigate the effect of operation conditions [7].

Although silica-PEI adsorbents have received considerable attention as the leading candidate of strong basic adsorbents for post-combustion capture, no detailed performance evaluation under specific conditions has been reported except for a few pilot studies [8–11]. We extend our previous study [7] to evaluate the CO_2 capture performance of the silica-PEI adsorbent, on a 100 kg scale over 150 hour continuous operation under various operating conditions in a fluidized bed continuous unit. This represents a 20-fold increase in scale compared to the TBS

study reported previously [7]. Firstly, continuous operation was carried out for 100 h in the sorption reactor with where gas velocity, inlet CO_2 concentration, temperature, and the differential pressure were varied. Secondly, continuous operation was continued for a further 50 h in the sorption reactor with varying the inlet H_2O concentration, in addition to the temperature and inlet CO_2 concentration.

2. Experimental

2.1 Material

UNOTT prepared the silica-PEI adsorbent for post-combustion CO_2 capture for testing at KIER. Kim et al. previously evaluated the CO_2 capture performance on two types of silica-PEI adsorbents with different PEI molecular masses in a TBS [7]. The physical properties of the fresh adsorbent (S.PEI-5K) used here can be found in our previous study [7]. (Average particle size : 240 μm, Particle distribution : 80 ~ 498 μm, bulk density : 0.5512 g/cm^3)

2.2 Apparatus

The 100 kg scale fluidized bed continuous unit was designed for post-combustion CO_2 capture using solid adsorbents. Figure 1 shows the schematic diagram of the unit. It mainly consists of a bubbling fluidized-bed type sorption reactor, a bubbling fluidized-bed type desorption reactor, and a cyclone for separating gas and solids. For solids handling, a transport system was placed to circulate adsorbents from the sorption reactor to the desorption one and the solid circulation

rate was controlled by manipulating revolutions per minute (rpm) of the rotary valve. A gas recirculation system for the CO_2 gas discharged from the desorption reactor has been installed in order to maintain high CO_2 purity. For heat control, a steam generator supplies energy to the desorption reactor in order to heat adsorbents and supply heat of reaction. An auto chiller (HYUNDAI ENG Co. Ltd., Korea) was used for the cooling adsorbent and removing heat of reaction in the sorption reactor. An IR gas analyzer (ABB, Advance Optima, Switzerland) was used to measure CO_2 concentration for the inlet and outlet gas streams of each reactor.

(Figure 1)

The bubbling fluidized-bed sorption reactor had a width of 0.3 m, a length of 0.3 m and a height of 3.0 m. The heat of reaction generated in the sorption reactor, was dissipated by controlling by the inlet temperature and the flowrate of the cooling water through the heat exchanger horizontally installed in the reactor. In front of the sorption reactor, a bubbler producing water vapor at a specific temperature was installed to control the amount in the simulated flue gas. A line heater was installed in the gas flow line from the rear end of the bubbler to the sorption reactor in order to increase the temperature of the gas stream and to prevent water vapor condensation in the gas stream. The simulated flue gas, introduced into the sorption reactor, was a mixture of N_2 (99.999%), CO_2 (99.99%) and H_2O, which was determined based on the experimental conditions.

The bubbling fluidized-bed type desorption reactor had a width of 0.35 m, a length of 0.35 m and a height of 3.0 m. Steam was injected into a heat exchanger horizontally installed in the

reactor in order to supply the endothermic heat of reaction. In order to prevent solids bypassing the desorption reactor, a partition was installed between the solid inlet and outlet port. In front of the desorption reactor, a bubbler was also installed to control the amount of water vapor fed into the reactor. Zhang et al. reported that the adsorption capacity has been stabilized when the same amount of water vapor as the sorption reactor is fed into the desorption reactor [28]. A preheater was installed at the rear end of the bubbler to maintain temperature high enough in the gas stream in order to prevent water vapor condensation in the gas stream. A simulated gas or recirculated gas from the desorption reactor has been used as the fluidizing gas in the desorption reactor. Firstly, simulated gas of mixtures of N_2 (99.999%) and CO_2 (99.99%) with water vapor were used. Secondly, the gas stream discharged from the desorption reactor was recirculated by a gas recirculation pump. To control CO_2 concentration in the desorption reactor, a certain amount of pure CO_2 (99.99%) was added to this gas stream.

The solid transport system consists of a fast fluidized-bed reactor with a total height of 8.0 m. A perforated plate was installed as the gas distributor. Air as a fluidizing gas was used to transport the solid particles to the main cyclone. The gas and solids are separated in the main cyclone and the separated solids are introduced into the desorption reactor. The solids, introduced into the desorption reactor, are regenerated before being supplied to the sorption reactor. The solids, introduced into the sorption reactor, adsorb CO_2 before being supplied to the solid transport system. The solid circulation rate was controlled by manipulating the rotational speed of the rotary valve installed between the sorption reactor and the solid transport system. The gas flow rate of each component, such as N_2 and CO_2, was controlled using an MFC (mass flow controller, E5850, Brooks instruments). The RTD (Resistor Temperature Detector) was installed in each reactor and gas and solid flow line so that the temperature of

each point was measured. A pressure gauge and a differential pressure gauge were installed to investigate the fluidization state in the reactor and gas flow conditions. The humidity of the gas stream was measured using a thermo-hygrometer installed at the front and rear of each reactor. In addition, an IR gas analyzer was installed to measure CO_2 concentration before and after the reaction in real time. Measured values from all instruments (thermometer, differential pressure gauge, analyzer, etc.), installed in the 100 kg scale fluidized bed continuous unit, were collected through PLC (Programmable Logic Controller).

2.3 Conditions and Methods

Experimental parameters measured in the continuous operation for the first 100 h without introducing water vapor into the sorption reactor were as follows: 1) the gas velocity in the sorption reactor, 2) the inlet CO_2 concentration in the desorption reactor, 3) the temperature of the sorption reactor, 4) the inlet CO_2 concentration in the sorption reactor and 5) the differential pressure of the sorption reactor. The next 50 h was with water vapor introduced into the sorption reactor with the concentration being measured. The experimental conditions used for the 150 h continuous test are summarized in Table 1.

(Table 1)

The 100 kg batch of the S.PEI-5K adsorbent was charged into the unit through the desorption reactor under fluidization. After charging the adsorbent, the gas velocities for the solid transporting system were set to 1.60 m/s for the sorption reactor and 3.8 cm/s for the desorption

reactor. The solids circulation rate, which was manipulated by varying the rotational speed of the rotary valve between the desorption and sorption reactors, was calculated by the increase of the bed differential pressure in the sorption reactor or the decrease of that in the desorption reactor. During solids circulation, the desorption reactor was heated to the reaction temperature of 129–130°C. The experiment was started after the adsorbent was dried and regenerated for 12 h at the reaction temperature with the solids circulation rate of 62.4 kg/h.

During continuous operation, all the inlet and outlet gas streams from the sorption and the desorption reactor were analyzed using the on-line IR gas analyzer (ABB, Advance Optima, Switzerland). The amount of CO_2 sorbed was calculated from the CO_2 concentrations to obtain the CO_2 removal efficiency in the sorption reactor. The dynamic sorption capacity of the sorbents was calculated from the amount of CO_2 sorbed and the solid circulation rate. Based on the CO_2 removal efficiency and the dynamic sorption, the sorbent performance was evaluated with respect to the changes in the experimental conditions.

The adsorbents were sampled from the bottom of the sorption and desorption reactors during the test. The list of the samples analyzed are summarized in Table 2. The physical and chemical characteristics of each sample (SP-F, SP-S and SP-D) were analyzed by a thermogravimetric analyzer (TGA, SDT Q-600), NMR. The weight loss of the samples were examined using a thermogravimetric analyzer manufactured by TA at the temperature range from 30°C to 130°C in N_2 atmosphere. ^{13}C-NMR data were acquired on 400 MHz Solid State NMR spectrometer (AVANCE III HD, Bruker, Germany) at Korea Basic Science Institute, Seoul Western Center. ^{13}C CP/MAS NMR measurement was performed at a Larmor frequency of 100.66 MHz. Samples were placed in a 4 mm CP/MAS probe, and the spinning rate was set to 10 kHz in order to minimize spinning-sideband overlap. The isobaric CO_2 uptake of samples (SP-F, SP-

A1 and SP-A2) were evaluated using 15% CO_2 in nitrogen byTGA and in a xxx apparatus using CO2 partial pressures up to 1 bar. BET. Each sample was pretreated for a day at each regenerable temperature (130ºC) and then the isothermal CO_2 uptake for samples was compared at both the adsorption temperature (70ºC) and various CO_2 partial pressures (0–1 bar).

Commented [CS1]: Name of instrument. Note BET refers to multi-layer adsorption. Only mono-layer for CO2 since carbamate complex formed.

Formatted: Subscript

(Table 2)

Results and discussion

3.1. 150-hour continuous operation with various experimental conditions

Figure 2 presents the results for 100 kg of the S.PEI-5K in the fluidized bed continuous unit. Figure 2(a) shows the CO_2 removal efficiency and the dynamic sorption capacity of the adsorbent. Figure 2(b) shows the CO_2 concentrations at the inlet and outlet stream of the sorption and desorption reactor. Up to 67 h, the inlet CO_2 concentration of the sorption reactor was maintained at 21.0–21.2 vol.%. After 67 h, the inlet CO_2 concentration of the sorption reactor was changed from 13.6 to 18.7 vol.%. After 90 h, the inlet CO_2 concentration of the sorption reactor was maintained at 18.9–21.0 vol.% until 143 h, after which the inlet CO_2 concentration was changed to 12.3 vol.%.

CO_2 was not introduced into the desorption reactor until after 41 h where the inlet CO_2 concentration was then set to 29.8 vol.% using a boosting fan for recirculating the gas

discharged from the desorption reactor. Between 90 and 126 h, CO_2 was introduced into the desorption reactor after which the CO_2 concentration (CO_2 purity) in the desorption reactor was set to be above 80 vol.%.

Figure 2(c) shows the H_2O concentration for the inlet and outlet streams of the sorption and desorption reactors. As already stated, H_2O was not introduced into the sorption reactor until 100 h where it was set to 8.3 vol.%, with the inlet H_2O concentration of the sorption reactor was maintained in the range 7.9–8.3 vol.% between 105 and 150 h operation. For the first 90 h, the H_2O concentration at the inlet of the desorption reactor was maintained at 12–14 vol.%. After 90 h, it was changed from 11.5 to 8.0 vol.% and then maintained at 8.5–8.8 vol.% between 105 and 150 h.

Figure 2(d) shows the temperature profiles of the sorption and desorption reactors. During the first 90 h, the temperature of the desorption reactor was stable at 130°C. The temperature of the sorption reactor was maintained at 68–70°C and after 60 h was varied between 50 and 69°C. After 75 h, the temperature was maintained at 69–70°C until 107 h and manipulated to the temperature range of 50–70°C. After 140 h, the temperature was maintained at 50-51°C. Figure 2(e) shows the bed differential pressure profiles of the sorption and desorption reactors. These were stable up to 83 h after which the bed differential pressure for the sorption reactor was changed from 357 to 176 mmH_2O that for the desorption reactor was changed from 475 to 580 mmH_2O. After 90 h, the bed differential pressures of the sorption reactor and the desorption reactor were again stable until the continuous test was completed.

Between 100 and 107 h, the changes in the inlet H_2O concentration to the sorption reactor at 70°C are presented in Table 1 (nos. 21, 22, 23 and 24), together with the other experimental conditions for this experiment. The sorption performance did not change much when the inlet

H_2O concentration of the sorption reactor was increased from 0 to 3.1, 5.9, and 8.3 vol.% with the CO_2 removal efficiency and the dynamic sorption capacity maintained at 81.5% and 6.42 wt.%, respectively. Between 107 to 122 h, the inlet H_2O concentration to the sorption reactor was 8.2 vol.% where Table 1 lists the condition used (nos. 25-28) As the temperature was increased to 50, 55, 61, 65 and 70°C, the sorption performance of sorbents did not change to a significant extent, unlike under dry conditions. Between 50 and 70°C with wet gas, the CO_2 removal efficiency and a dynamic sorption capacity were above 80% and 6.5 wt.%, respectively.

(Figure 2)

3.1.1. Change of the gas velocity in the sorption reactor

The conditions used for this experiment are nos. 1-4 in Table 1. Figure 3 shows the experimental results according to the change of gas velocity in the sorption reactor under dry gas conditions. Figure 3(a) shows the temperature of the sorption reactor with varying the inlet gas velocity. The temperature measured at different bed heights was different at gas velocities below 5.1 cm/s, but it became similar at higher gas velocities, indicating that solid particles were well fluidized. Figure 3(b) shows the CO_2 removal efficiency and the dynamic sorption capacity of adsorbents according to the change of gas velocity in the sorption reactor. The CO_2 removal efficiency decreased to 98.6, 95.6, 86.5 and 69.1% as the gas velocity in the sorption reactor was increased to 3.8, 4.5, 5.1 and 6.2 cm/s, respectively. The dynamic sorption capacity increased to 6.29, 7.57 and 7.90 wt.% as the gas velocity increased to 3.8, 4.5 and 5.1 cm/s, respectively, whereas it has been reduced slightly from 7.90 to 7.78 wt.% when the gas velocity

increased from 5.1 to 6.2 cm/s. When the gas velocity increased, the inlet CO_2 flow rate increased so that the sorption capacity may decrease. Since the sorption performance of adsorbents was the best when the gas velocity was 5.1 cm/s based on the experimental results, the optimum gas velocity in the sorption reactor has been set to this value.

(Figure 3)

3.1.2. Change of the temperature in the sorption reactor under dry conditions

The sorption performance has been investigated between 50 and 70ºC since the operating temperature of the FGD (flue gas desulfurization) unit, typically installed right before CO_2 capture process, is around 50-60ºC and the optimum sorption temperature of PEI adsorbents is 70ºC [28]. Nos 6, 8, 9, 10 and 11 listed in Table 1 were the experimental conditions in this experiment. Figure 4 shows the experimental results according to the temperature change in the sorption reactor when the inlet CO_2 concentration of the sorption reactor is 21.1 vol.% and the inlet CO_2 concentration of the desorption reactor is 29.8 vol.%. As the temperature of the sorption reactor increased to 50, 56, 60, 65 and 69ºC, the CO_2 removal efficiency increased to 60.0, 61.8, 64.7, 65.2 and 65.6%, and the dynamic sorption capacity increased to 5.34, 5.50, 5.72, 5.79 and 5.81 wt.%, respectively. The performance of the sorbents significantly increased over the temperature range of 50–60ºC, followed by a further slight increase as the temperature increased above 60ºC. This confirms that the proportional increase in the sorption performance reduces as the temperature approaches the optimum sorption temperature based on CO_2 uptake for silica-PEI, reported by Zhang et al [28].

(Figure 4)

3.1.3. Change of the inlet CO_2 concentration of the sorption reactor

Experiments have been carried out by varying the inlet CO_2 concentration of the sorption reactor under the same operating conditions. Nos 12, 13, 14, 15 and 16 listed in Table 1, were the experimental conditions used in this experiment. Figure 5 shows the experimental results according to the change of the inlet CO_2 concentration to the sorption reactor. When the inlet CO_2 concentration increased to 13.6, 14.9, 16.0, 17.4, and 18.7 vol.%, the CO_2 removal efficiency decreased to 87.0, 80.6, 76.1, 69.6 and 66.5%, while the dynamic sorption capacity increased to 5.58, 5.62, 5.64, 5.66 and 5.76 wt.%, respectively. Thus, the CO_2 removal efficiency decreased markedly while the dynamic sorption capacity of sorbents slightly increased. According to the CO_2 partial pressure, the amount of captured CO_2 increased slightly giving a small increase in sorption capacity. However, when the inlet CO_2 concentration increased, the CO_2 removal efficiency decreased at a fixed solid circulation rate. As the amount of solids in the sorption reactor is constant since the solid circulation rate is constant, the amount of CO_2 removed per mass of adsorbent in the sorption reactor increased. Thus, the CO_2 removal efficiency is reduced even if the CO_2 uptake generally increases with increasing CO_2 partial pressure. Considering the of CO_2 removal efficiency is over 80% under the given operating conditions, the inlet CO_2 concentration in the sorption reactor for the stable operation can range from 13.6 to 15.0 vol.%.

(Figure 5)

3.1.4. Change of the bed height in the sorption reactor

In the experiment, the gas-solid contact time can be calculated from the gas velocity and the bed height, which can be known through the differential pressure of the reactor. Nos 12, 17, 18, 19 and 20 listed in Table 1 were the experimental conditions. When the differential pressure of the reactor increased, the bed height in the reactor increased, and vice versa. As the differential pressure of the sorption reactor increased to 176, 204, 234, 270, and 357 mmH_2O, the gas-solid contact time increased to 5.8, 6.7, 7.6, 8.8, and 11.5 sec. Figure 6 shows that when the gas-solid contact time increased to 5.8, 6.7, 7.6, 8.8 and 11.5 sec, the CO_2 removal efficiency increased to 74.2, 77.1, 80.2, 81.9, and 87.0%, and the dynamic sorption capacity increased to 4.75, 4.92, 5.10, 5.26 and 5.58 wt.%, respectively. Zhang et al. reported that an increase in gas-solid contact time by increasing bed material in the reactor can effectively increased the dynamic adsorption capacity, but it will also increase the amount of solid inventory in the reactor and the size of reactor required, leading to higher capital and operational costs [27]. Based on the experimental results, the CO_2 sorption performance was the best when the gas-solid contact time was 11.5 sec. However, it will be change when the CO_2 purity for the desorption reactor is higher since the working capacity of the S.PEI adsorbent decreased when the CO_2 partial pressure of above 0.8 [28].

(Figure 6)

3.1.5. Change of the inlet CO_2 concentration to the desorption reactor

For practical applications, steam or pure CO_2 has to be introduced to the desorption reactor to achieve high CO_2 purity [47]. Thus, the CO_2 removal efficiency and the dynamic sorption capacity of adsorbents should be evaluated under the desorption conditions that take into account high CO_2 partial pressures in the desorption reactor. The sorption performance has been investigated according to the change of the CO_2 partial pressure at different inlet H_2O concentrations for the sorption reactor. The inlet CO_2 concentration of the desorption reactor was changed for the conditions in the sorption reactor under dry gas. Nos 3, 5, 6 and 7 listed in Table 1 were the experimental conditions in this experiment. The inlet CO_2 concentration has been adjusted from 0 to 45 vol.% by manipulating the N_2 and CO_2 flowrates into the desorption reactor. However, there was a limit to increase CO_2 concentration using the MFC used in the study. Higher CO_2 was carried out using a gas recirculation pump for recirculating the gas, discharged from the desorption reactor under the wet gas condition in the sorption reactor. Nos 29, 30, 31 and 32 shown in Table 1 were the experimental conditions in this experiment.

Figure 7 shows the results according to the change of the inlet CO_2 concentration to the desorption reactor. Figure 7(a) shows the CO_2 removal efficiency and the dynamic sorption capacity according to the change of the inlet CO_2 concentration to the desorption reactor. As the inlet CO_2 concentration of the desorption reactor increased from zero to 14.6, 29.8, 45.0 vol.% under dry gas conditions, the CO_2 partial pressure of the desorption reactor increased while the CO_2 removal efficiency and the dynamic sorption capacity of adsorbents gradually decreased. Figure 7(b) shows the CO_2 purity at the outlet stream of the desorption reactor according to the change of the inlet CO_2 concentration to the desorption reactor. In continuous operation with dry gas in the sorption reactor, the CO_2 purity at the outlet stream of the

desorption reactor was 53 vol.% when the inlet CO_2 concentration of the desorption reactor was 45 vol.%. As the inlet CO_2 concentration of the desorption reactor increased to 0, 26.3, 60.2, and 81.2 vol.% under wet gas conditions, the CO_2 purity of the desorption reactor increased while the CO_2 removal efficiency and the dynamic sorption capacity of adsorbents decreased. The CO_2 removal efficiency and the dynamic sorption capacity of adsorbents were 46.5% and 3.64 wt.%, respectively, when the CO_2 purity of the desorption reactor was 83.3 vol.%. Zhang et al. also reported that the working capacity decreased with an increase in CO_2 partial pressure at the actual desorption CO_2 partial pressure of above 0.8, which eventually increased the weight uptake of the amine-supported adsorbents [28]. They also demonstrated a detrimental effect of CO_2 in the stripping gas on the cyclic performance of the PEI/silica adsorbent [29]. In this study, this was confirmed by TG analysis of solid particles sampled during the continuous operation in a desorption reactor under wet gas conditions.

(Figure 7)

3.2. Property analysis of the sorbent samples

Figure 8 shows the TGA results of the sorbent samples. (SP1-4). The experimental conditions used when SP1, SP2, SP3 and SP4 samples were collected were Nos 1, 3, 28 and 33 listed in Table 1, respectively. The weight loss of the sorbent sample was related to the amount of CO_2 sorbed in the sorption reactor while that of the sample after desorption was the amount of CO_2 remaining. Figure 8(a) shows the results for the samples after sorption (SP1-4-S) where each sample displays a similar weight loss up to 90°C, and then showed a difference in weight loss

at 130°C. Figure 8(b) shows the TGA results for the sample before reaction (SP-F) and the sample after desorption (SP-D). The fresh sorbent showed a weight loss is less than 2.0 wt.% up to 130ºC due to moisture with the greatest weight loss occurring between 80 and 100ºC. The samples after desorption, SP1-D, SP2-D and SP3-D showed a similar weight loss of less than 2.5 wt.% up to 130ºC. There is no significant difference in weight loss compared with the fresh sorbent. From this, it can be concluded that the virtual complete desorption of CO_2 was achieved at the given operating conditions that SP1-D, SP2-D, and SP3-D had been collected. However, SP4-D showed a rapid weight loss about 4.5 wt.% up to 130ºC. Therefore, the desorption ability has been reduced at the given operating conditions that SP4-D has been collected. In Figure 8(a), when SP1-S and SP2-S are compared, SP2-S showed greater weight loss than SP1-S. This means that the amount of CO_2 sorbed on SP2-S is higher than that of SP1-S. In Figure 8(b), SP1-D and SP2-D showed similar weight loss up to 130°C meaning that the CO_2 sorption ability of sorbent was higher at the given operating conditions that SP2-S and SP2-D have been collected. Compared SP3-S and SP4-S in Figure 8(a), SP3-S and SP4-S shows similar weight loss up to 130°C. However, in Figure 8(b), SP4-D shows a greater weight loss than in SP3-D. This can be explained that the higher the CO_2 partial pressure, the lower the desorption ability of the sorbents.

(Figure 8)

The dynamic sorption capacity of each sample was calculated from TGA. In order to consider only the amount of CO_2, the amount of H_2O in total weight loss in TGA was removed based on the H_2O/CO_2 molar ratio sorbed by the absorbent in each experimental condition. As shown

in Figure 9, the dynamic sorption capacities using continuous experimental data for SP1, SP2, SP3 and SP4 were calculated as 6.29, 7.90, 6.46 and 3.34 wt.%, respectively, and that using the TGA data was 6.25, 7.86, 6.22 and 2.84 wt.%, respectively. Thus, the dynamic sorption capacity from the continuous experimental data is in close agreement with from the TGA data. Moreover, when 52.4 vol.% of CO_2 was injected into the desorption reactor under the experimental conditions SP4, the dynamic sorption capacity was significantly reduced relative to the other experimental conditions.

(Figure 9)

To elucidate chemical reactions between CO_2 and PEI in silica, we performed solid state ^{13}C-NMR analysis of silica-PEI obtained from adsorption and desorption of the fluidized bed continuous unit. As shown in Figure 10(a), characteristic carbon peaks of branched PEI in silica were observed (δC 20.1 – 70.5 ppm) from ethylene moieties. After CO_2 adsorption at the condition of SP1-S (w/o H_2O), ethylene peaks became a broad single peak, and a new single peak appeared at 164 ppm, representing carbamate formation [48]. Following regeneration, at the conditions used for SP1-D, ^{13}C-NMR data showed the pronounced decrease in the carbamate peak and recovery of the ethylene peaks at the upfield position. The relatively small amount of carbamate remaining could arise from CO_2 being adsorbed from the atmosphere prior to analysis, given that TG has suggested that virtually complete desorption was achieved for this sample. As shown in Figure 11(a), with injection of H_2O in sorption process of the fluidized bed continuous unit, carbamate formation was also confirmed by ^{13}C-NMR data. However, when CO_2 (52.4 vol.%) was injected to the desorption reactor under a condition of

SP4-D, there are no notable change in the ethylene and carbamate peak intensities because of presence of CO_2 during desorption process (Figure 11(b)). This is qualitatively consistent with the low dynamic sorption capacity calculated for this sample (Figure 9).

(Figure 10)

(Figure 11)

3.3. Isothermal CO_2 uptakes for silica-PEI adsorbents using the BET

The CO_2 sorption performance of adsorbent samples were evaluated by BET where the isothermal CO_2 uptakes at an adsorption temperature (70°C) and various CO_2 partial pressures (0–1 bar) have been compared. The three types of adsorbent samples named as SP-F, SP-A1 and SP-A2 were used in the BET test. SP-F represents the fresh adsorbent, SP-A1 represents the adsorbent sampled from the reactor after operation for 90 h whereas SP-A2 was sampled after completion that a 150-hour continuous operation. Figure 12 shows isothermal CO_2 uptakes at different CO_2 partial pressures with the constant temperature of 70ºC using BET. At the CO_2 partial pressure used (0.15 bar) for the post-combustion flue gas, the CO_2 uptake of silica-PEI samples was 8.67 (SP-F), 7.31 (SP-A1) and 5.84 (SP-A2) wt.%, respectively. The CO_2 sorption performance of the adsorbents decreased with increasing run time and it can be summised that oxidative degradation of PEI occurred due to the oxygen in the air flowing into the solid transportation system in the continuous experiment, together with the adsorber operating dry for the first 100 h of testing. Calleja et al. [49] discovered that the supported

amines oxidize in air under typical drying conditions. They reported that CO_2 sorption performance of amine grafted on SBA-15 silica with various drying time at 20ºC and 110ºC in air was decreased gradually with air treatment duration and increasing drying time [49]. Bali et al. investigated the oxidative deactivation of branched PEI- and PAA-impregnated mesoporous γ-alumina using treatment for 24 h in the O_2 concentration of 5 vol.% and 21 vol.% in N_2 at 70 and 110ºC, reporting that higher O_2 levels and higher treatment temperatures significantly increased the extent of air oxidation [50]. In the continuous experiment here, the adsorbent was contacted with air for long time at a high concentration of oxygen, which has led to a decrease in the CO_2 sorption performance due to oxidative degradation of PEI during continuous operation.

(Figure 12)

Conclusions

The gas velocity required for good fluidization in a bubbling fluidized-bed type sorption reactor was above 5.1 cm/sec and the CO_2 sorption performance of the adsorbents was the best when the gas velocity was 5.1 cm/s. CO_2 removal efficiencies of over 905% with dynamic sorption capacities of ~~above~~ 7.50 wt.% have been achieved. The sorption performance was not significantly affected by the change of the inlet H_2O concentration (3.1-8.3 vol.%) in the sorption reactor and it was maintained well at even below 60ºC, which is close to the coal-fired flue gas temperature (55-60ºC) after flue gas desulfurization (FGD). As the bed height in the sorption reactor was raised, the sorption performance as well as the dynamic sorption capacity

of the adsorbent increased due to the longer gas-solid contact time.

The sorption performance of the adsorbent decreased when the CO_2 partial pressure of the desorption reactor increased and it was confirmed that the adsorbent has been degraded as the continuous operating time increased. Therefore, for long-term operation and to achieve efficient CO_2 sorption performance, further studies are needed to demonstrate that moisture throughout the system will mitigate against oxidation and effective regeneration at high CO_2 partial pressures is feasible in the move to commercialization of CO_2 capture processes using PEI-based solid adsorbents.

Acknowledgement

This work was supported by the Korea Institute of Energy Technology Evaluation and Planning (KETEP) and the Ministry of Trade, Industry & Energy (MOTIE) of the Republic of Korea (No. 20158510011280). The University of Nottingham also acknowledges financial support from the Engineering and Physical Sciences Research Council (grant number EP/P026214/1), as part of the UK CCS Research Centre.

References

[1] J.-Y. Kim, H. Lim, J.M. Woo, S.-H. Jo, J.-H. Moon, S.-Y. Lee, H. Lee, C.-K. Yi, J.-S. Lee, B.-M. Min, Y.C. Park, Performance evaluation of K-based solid sorbents depending on the internal structure of the carbonator in the bench-scale CO_2 capture process. Korean Chem. Eng. Res. 55 (2017) 419–425.

[2] Y.C. Park, S.-H. Jo, S.-Y. Lee, J.-H. Moon, C.-K. Ryu, J.B. Lee, C.-K. Yi, Performance analysis of K-based KEP-CO2P1 solid sorbents in a bench-scale continuous dry-sorbent CO_2 capture process. Korean J. Chem. Eng. 33 (2016) 73–79.

[3] H. Nam, Y. Won, J.-Y. Kim, C.-K. Yi, Y.C. Park, J.M. Woo, S.-Y. Jung, G.-T. Jin, S.-H. Jo, S.-Y. Lee, H. Kim, J. Park, Hydrodynamics and heat transfer coefficients during CO_2 carbonation reaction in a circulated fluidized bed reactor using 200 kg potassium-based dry sorbent. Energy 193 (2020) 116643.

[4] Y.C. Park, S.-H. Jo, C.-K. Ryu, C.-K. Yi, Demonstration of pilot scale carbon dioxide capture system using dry regenerable sorbents to the real coal-fired power plant in Korea. Energy Procedia 4 (2011) 1508–1512.

[5] Y.C. Park, S.-H. Jo, D.H. Lee, C.-K. Yi, C.K. Ryu, K.S. Kim, C.H. You, K.S. Park, The status of the development project for the 10 MWe-scale dry-sorbent carbon dioxide capture system to the real coal-fired power plant in Korea. Energy Procedia 37 (2013) 122–6.

[6] Y.C. Park, S.-H. Jo, D.-H. Kyung, J.-Y. Kim, C.-K. Yi, C.K. Ryu, M.S. Shin, Test operation results of the 10 MWe-scale dry-sorbent CO_2 capture process integrated with a real coal-

fired power plant in Korea. Energy Procedia 63 (2014) 2261–2265.

[7] J.-Y. Kim, J.-M. Woo, S.-H. Jo, S.-Y. Lee, J.-H. Moon, H. Kim, C.-K. Yi, H. Lee, C.E. Snape, L. Stevens, C. Sun, H. Liu, J. Liu, Park, Y.C. Park, Continuous testing of silica-PEI adsorbents in a lab.-scale twin bubbling fluidized-bed system. Int. J. Greenh. Gas Control 82 (2019) 184–191.

[8] T.O. Nelson, A. Kataria, P. Mobley, M. Soukri, J. Tanthana, RTI's solid sorbent-based CO_2 capture process: technical and economic lessons learned for application in coal-fired, NGCC, and cement plants. Energy Procedia 114 (2017) 1536–1545.

[9] H. Krutka, S. Sjostroma, T. Starnsa, M. Dillona, R. Silvermanb, Post-combustion CO_2 capture using solid sorbents: 1 MWe pilot evaluation. Energy Procedia 37 (2013) 73–88.

[10] W.J. Morris, S. Sjostrom, M. Sayyah, J. Denney, O. Syed, C. Lindsey, M. Lindsay, ADA's solid sorbent CO_2 capture process: developing solid sorbent technology to provide the necessary flexible CO_2 capture solutions for a wide range of applications. Energy Procedia 63 (2014) 1536–1545.

[11] S. Sjostrom, C. Senior, 2019. Pilot testing of CO_2 capture from a coal-fired power plant–Part 1: Sorbent characterization. Clean Energy 3 (2019) 144–162 and 4 (2020) 12-25.

[12] P.J.E. Harlick, A. Sayari, Applications of pore-expanded mesoporous silicas. 3. Triamine silane grafting for enhanced CO_2 adsorption. Ind. Eng. Chem. Res. 45 (2006) 3248–3255.

[13] P.J.E. Harlick, A. Sayari, Applications of pore-expanded mesoporous silica. 5. Triamine grafted material with exceptional CO_2 dynamic and equilibrium adsorption performance, Ind. Eng. Chem. Res. 46 (2007) 446–458.

[14] R. Serna-Guerrero, Y. Belmabkhout, A. Sayari, Further investigations of CO_2 capture using triamine-grafted poreexpanded mesoporous silica, Chem. Eng. J. 158 (2010) 513–519.

[15] R. Serna-Guerrero, Y. Belmabkhout, A. Sayari, Influence of regeneration conditions on the cyclic performance of amine-grafted mesoporous silica for CO_2 capture: an experimental and statistical study, Chem. Eng. Sci. 65 (2010) 4166–4172.

[16] Y. Belmabkhout, R. Serna-Guerrero, A. Sayari, Amine bearing mesoporous silica for CO_2 removal from dry and humid air, Chem. Eng. Sci. 65 (2010) 3695–3698.

[17] A. Sayari, Y. Belmabkhout, R. Serna-Guerrero, Flue gas treatment via CO_2 adsorption, Chem. Eng. J. 171 (2011) 760–774.

[18] Sayari, Q. Liu, P. Mishra, Enhanced adsorption efficiency through materials design for direct air capture over supported polyethylenimine, ChemSusChem 9 (2016) 2796–2803.

[19] W. Chaikittisilp, H.J. Kim, C.W. Jones, Mesoporous alumina-supported amines as potential steam-stable adsorbents for capturing CO_2 from simulated flue gas and ambient air. Energy Fuels 25 (2011) 5528–5537.

[20] F. Rezaei, C.W. Jones, Stability of supported amine adsorbents to SO_2 and NOx in postcombustion CO_2 capture. 1. Single-component adsorption, Ind. Eng. Chem. Res. 52 (2013) 12192–12201.

[21] F. Rezaei, C.W. Jones, Stability of supported amine adsorbents to SO_2 and NOx in postcombustion CO_2 capture. 2. Multicomponent adsorption, Ind. Eng. Chem. Res. 53 (2014) 12103–12110.

[22] S.A. Didas, M.A. Sakwa-Novak, G.S. Foo, C. Sievers, C.W. Jones, Effect of amine surface coverage on the coadsorption of CO_2 and water: spectral deconvolution of adsorbed species, J. Phys. Chem. Lett. 5 (2014) 4194–4200.

[23] S.A. Didas, R. Zhu, N.A. Brunelli, D.S. Sholl, C.W. Jones, Thermal, oxidative and CO_2-induced degradation of primary amines used for CO_2 capture: effect of alkyl linker on stability, J. Phys. Chem. C 118 (2014) 12302–12311.

[24] A. Holewinski, M.A. Sakwa-Novak, C.W. Jones, Linking CO_2 sorption performance to polymer morphology in aminopolymer/silica composites through neutron scattering, J. Am. Chem. Soc. 137 (2015) 11749–11759.

[25] Holewinski, M.A. Sakwa-Novak, J.-M.Y. Carrillo, M.E. Potter, N. Ellebracht, G. Rother, B.G. Sumpter, C.W. Jones, Aminopolymer mobility and support interactions in silica-PEI composites for CO_2 capture applications: a quasielastic neutron scattering study, J. Phys. Chem. B 121 (2017) 6721–6731.

[26] W. Choi, K. Min, C. Kim, Y.S. Ko, J.W. Jeon, H. Seo, Y.-K. Park, M. Choi, Epoxide-functionalization of polyethyleneimine for synthesis of stable carbon dioxide adsorbent in temperature swing adsorption. Nat. Commun. 7 (2016) 12640.

[27] C. Kim, H.S. Cho, S. Chang, S.J. Cho, M. Choi, An ethylenediamine-grafted Y zeolite: a highly regenerable carbon dioxide adsorbent via temperature swing adsorption without urea formation. Energy Environ. Sci. 9 (2016) 1803–1811.

[28] K. Min, W. Choi, M. Choi, Macroporous silica with thick framework for steam-stable and high-performance poly(ethyleneimine)/silica CO_2 adsorbent. ChemSusChem 10 (2017) 2518-2526.

[29] K. Min, W. Choi, C. Kim, M. Choi, Oxidation-stable amine-containing adsorbents for carbon dioxide capture. Nat. Commun. 9 (2018) 726.

[30] K. Min, W. Choi, C. Kim, M. Choi, Rational design of the polymeric amines in solid adsorbents for postcombustion carbon dioxide capture, ACS Appl. Mater. Interfaces 10 (2018) 23825–23833.

[31] S. Park, K. Choi, H.J. Yu, Y.-J. Won, C. Kim, M. Choi, S.-H. Cho, J.-H. Lee, S.Y. Lee, J.K. Lee, Thermal stability enhanced tetraethylenepentamine/silica adsorbents for high performance CO_2 capture, Ind. Eng. Chem. Res. 57 (2018) 4632–4639.

[32] T.C. Drage, A. Arenillas, K.M. Smith, C.E. Snape, Thermal stability of polyethylenimine based carbon dioxide adsorbents and its influence on selection of regeneration strategies. Microporous Mesoporous Mater. 116, (2008) 504–512.

[33] T.C. Drage, C.E. Snape, L.A. Stevens, J. Wood, J. Wang, A.I. Cooper, R. Dawson, X. Guo, C. Satterley, R. Irons, Materials challenges for the development of solid sorbents for post-combustion carbon capture. J. Mater. Chem. 22 (2012) 2815.

[34] W. Zhang, H. Liu, C. Sun, T.C. Drage, C.E. Snape, Performance of polyethyleneimine–silica adsorbent for post-combustion CO_2 capture in a bubbling fluidized bed. Chem. Eng. J. 251 (2014) 293–303.

[35] W. Zhang, H. Liu, Y. Sun, J. Cakstins, C. Sun, C.E. Snape, Parametric study on the regeneration heat requirement of an amine-based solid adsorbent process for post-combustion carbon capture. Applied Energy 168 (2016) 394–405.

[36] W. Zhang, C. Sun, C.E. Snape, X. Sun, H. Liu, Cyclic performance evaluation of a

polyethylenimine/silica adsorbent with steam regeneration using simulated NGCC flue gas and actual flue gas of a gas-fired boiler in a bubbling fluidized bed reactor. Int. J. Greenh. Gas Control 95 (2020) 102975.

[37] C.-K. Yi, S.W. Hong, S.-H. Jo, J.E. Son, J.H. Choi, Absorption and regeneration characteristics of a sorbent for fluidized-bed CO_2 removal process. Korean Chem. Eng. Res. 43 (2005) 294–298.

[38] C.-K. Yi, S.-H. Jo, Y. Seo, K.H. Moon, J.S. Yoo, CO_2 capture characteristics of dry sorbents in a fast fluidized reactor. Stud. Surf. Sci. Catal. 159 (2006) 501–504.

[39] C.-K. Yi, S.-H. Jo, Y. Seo, J.B. Lee, C.K. Ryu, Continuous operation of the potassium-based dry sorbent CO_2 capture process with two fluidized-bed reactors. Int. J. Greenh. Gas Control. 1 (2007) 31–36.

[40] C.-K. Yi, S.-H. Jo, Y. Seo, The effect of voidage on the CO_2 sorption capacity of K-based sorbent in a dual circulating fluidized bed process. J. Chem. Eng. Jap. 41 (2008) 691–694.

[41] C.-K. Yi, Advances of carbon capture technology. Korean Ind. Chem. News 12 (2009) 30–42.

[42] C.-K. Yi, Advances of post-combustion carbon capture technology by dry sorbent. Korean Chem. Eng. Res. 48 (2010) 140–146.

[43] Y.C. Park, S.-H. Jo, K.W. Park, Y.S. Park, C.-K. Yi, Effect of bed height on the carbon dioxide capture by carbonation/regeneration cyclic operations using dry potassium-based sorbents. Korean J. Chem. Eng. 26 (2009) 874–878.

[44] Y.C. Park, S.-H. Jo, C.K. Ryu, C.-K. Yi, Long-term operation of carbon dioxide capture

system from a real coal-fired flue gas using dry regenerable potassium-based sorbents. Energy Procedia 1 (2009) 1235–1239.

[45] K.-C. Kim, K.Y. Kim, Y.C. Park, S.-H. Jo, H.J. Ryu, C.-K. Yi, Study of hydrodynamics and reaction characteristics of K-based solid sorbents for CO_2 capture in a continuous system composed of two bubbling fluidized-bed reactors. Korean Chem. Eng. Res. 48 (2010) 499–505.

[46] K.-C. Kim, Y.C. Park, S.-H. Jo, C.-K. Yi, The effect of CO_2 or steam partial pressure in the regeneration of solid sorbents on the CO_2 capture efficiency in the two-interconnected bubbling fluidized-beds system. Korean J. Chem. Eng. 28 (2011) 1986–1989.

[47] H. Zhao, X. Luo, H. Zhang, N. Sun, W. Wei, Y. Sun, Carbon-based adsorbents for post-combustion capture: a review. Greenhouse Gas Sci. Technol. 8 (2018) 11–36.

[48] J.K. Moore, M.A. Sakwa-Novak, W. Chaikittisilp, A.K. Mehta, M.S. Conradi, C.W. Jones, S.E. Hayes, Characterization of a Mixture of CO_2 Adsorption Products in Hyperbranched Aminosilica Adsorbents by 13C Solid-State NMR. Environ. Sci. Technol. 49 (2015) 13684–13691.

[49] G. Calleja, R. Sanz, A. Arencibia, E.S. Sanz-Pe´rez, Influence of drying conditions on amine-functionalized SBA-15 as adsorbent of CO_2. Top. Catal. 54 (2011) 135–145.

[50] S. Bali, T.T. Chen, W. Chaikittisilpand C.W. Jones, Oxidative stability of amino polymer-alumina hybrid adsorbents for carbon dioxide capture. Energy Fuels 27 (2013) 1547–1554.

List of Tables

Table 1

NO.	Operation time (h)	Sorption reactor					Desorption reactor				Solid circulation rate (kg/h)
		Gas velocity (cm/s)	Inlet H_2O conc. (vol.%)	Inlet CO_2 conc. (vol.%)	Reactor temp. (^oC)	Differential pressure (mmH_2O)	Inlet H_2O conc. (vol.%)	Inlet CO_2 conc. (vol.%)	Reactor temp. (^oC)	Differential pressure (mmH_2O)	
1	0-41	**3.8***	-	20.0-21.5	68-69	350-370	12.0-13.5	-	129-130	450-460	62.4
2		**4.5***						-			
3		**5.1***						-			
4		**6.2***						-			
5	41-61	5.0-5.1	-	21.2-21.4	68-69	350-360	12.5-13.0	**14.6***	129-130	465-475	62.4
6								**29.8***			
7								**45.0***			
8	61-67	4.8-5.1	-	21.0-21.2	**65***	350-360	12.5-13.5	29.8	129-130	465-475	62.4
9					**60***						
10					**56***						
11					**50***						
12	74-83	5.0-5.1	-	**13.6***	67-68	360-370	12.5-13.5	29.88	129-130	460-475	56.1
13				**14.9***							
14				**16.0***							
15				**17.4***							
16				**18.7***							
17	83-90	5.0-5.1	-	13.6-13.7	67-68	**270***	12.5-13.0	29.8	129-130	520-580	56.1
18						**234***					

19						**204***					
20						**176***					
21			**-***					-			
22			**3.1***					-			
23	90-107906	5.0-5.5	**5.9***	19.5-20.5	69-70	360-370	8.0-11.5	-	129-130	450-460	70.9
24			**8.3***					-			
25					**65***			-			
26					**61***			-			
27	107-123	5.1-5.4	7.5-8.0	19.4-19.5	**55***	350-360	8.5-8.8	-	129-130	430-440	70.9
28					**50***			-			
29								**-***			
30								**26.3***			
31	123-143	5.3-5.4	7.5-8.0	18.8-18.9	69-70	350-370	8.5-8.8	**60.2***	129-130	445-465	66.1-70.9
32								**81.2***			
33	143-145	5.0-5.1	7.0-7.5	12.0-12.3	49-51	360-370	8.0-8.5	52.4	129-130	430-440	66.1

*** Change of condition**

Table 2

Sample name	Sorbent sampling point
SP-F	Fresh adsorbent
SP1-S SP1-D	After operation with condition of NO. 1
SP2-S SP2-D	After operation with condition of NO. 3
SP3-S SP3-D	After operation with condition of NO. 28
SP4-S SP4-D	After operation with condition of NO. 33
SP-A1	After continuous operation for 90 h
SP-A2	After continuous operation for 150 h

List of Figures

(SP4-D).

Figure 12. ~~BET results of I~~isobaric CO_2 uptake with temperature of 70ºC using various CO_2 partial pressure for the silica-PEI samples (fresh adsorbent and silica-PEI samples during continuous operation).

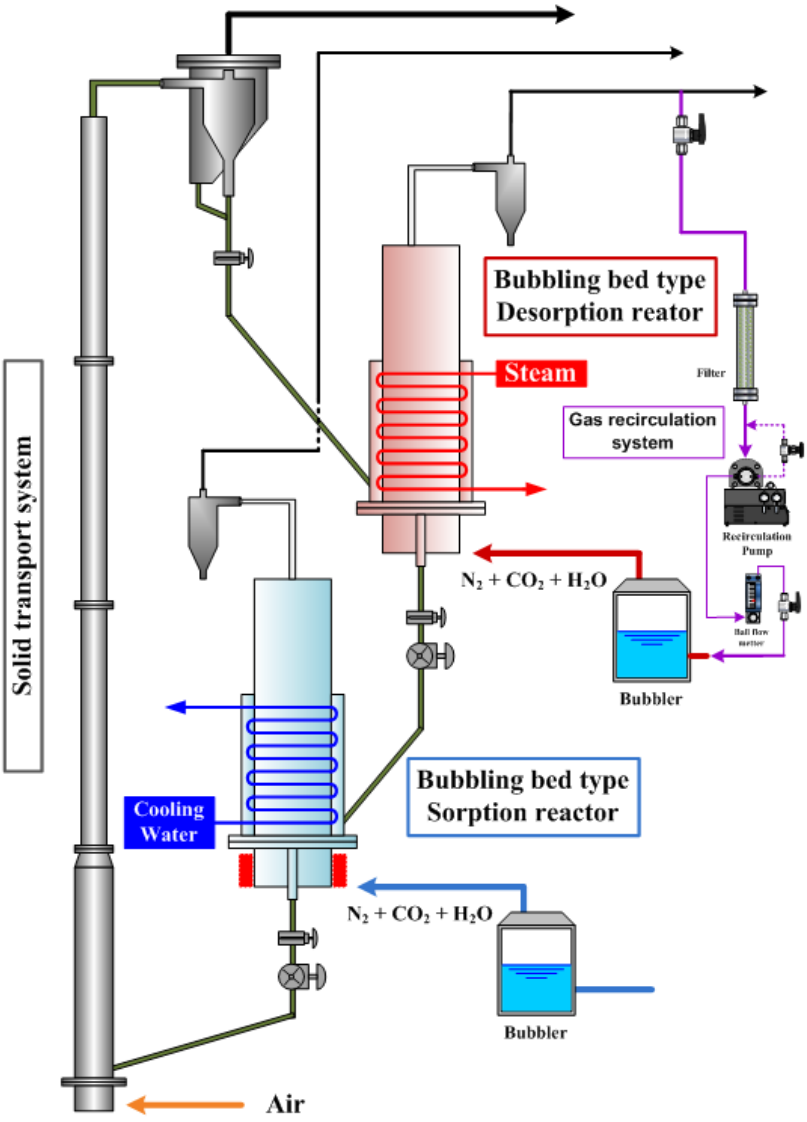
Solid transport system
Bubbling bed type
Desorption reator
Steam
Filter
Gas recirculation
system
Recirculation
Pump
$N_2 + CO_2 + H_2O$
Bubbler
Bubbling bed type
Sorption reactor
Cooling
Water
$N_2 + CO_2 + H_2O$
Bubbler
Air

Figure 1.

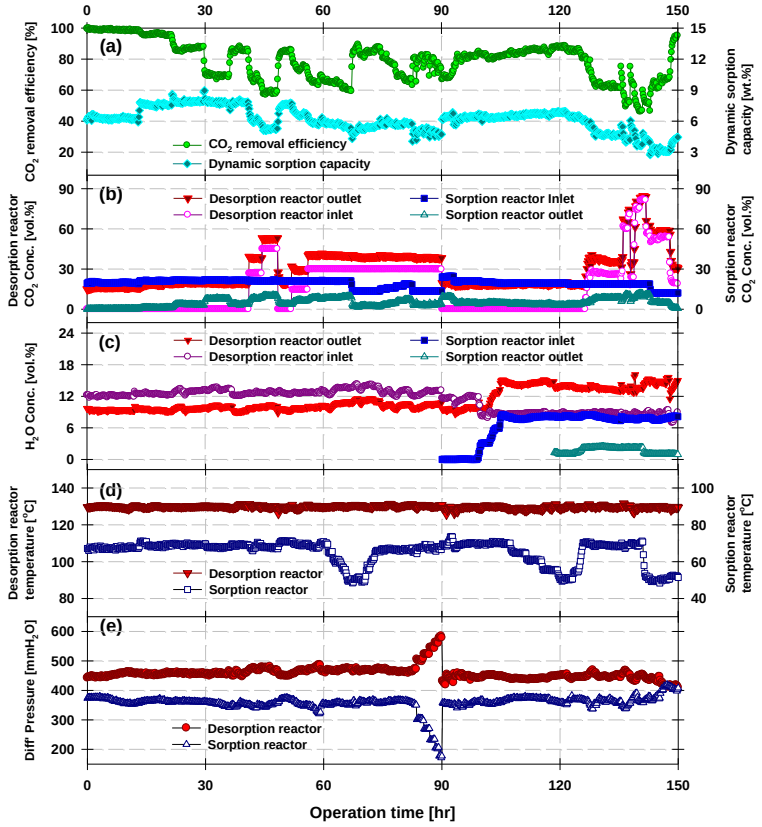
(a)
CO2 removal efficiency
Dynamic sorption capacity
CO2 removal efficiency [%]
Dynamic sorption capacity [wt.%]
(b)
Desorption reactor outlet
Desorption reactor inlet
Sorption reactor Inlet
Sorption reactor outlet
Desorption reactor CO2 Conc. [vol.%]
Sorption reactor CO2 Conc. [vol.%]
(c)
Desorption reactor outlet
Desorption reactor inlet
Sorption reactor inlet
Sorption reactor outlet
H2O Conc. [vol.%]
(d)
Desorption reactor
Sorption reactor
Desorption reactor temperature [°C]
Sorption reactor temperature [°C]
(e)
Desorption reactor
Sorption reactor
Diff Pressure [mmH2O]
Operation time [hr]

Figure 2.

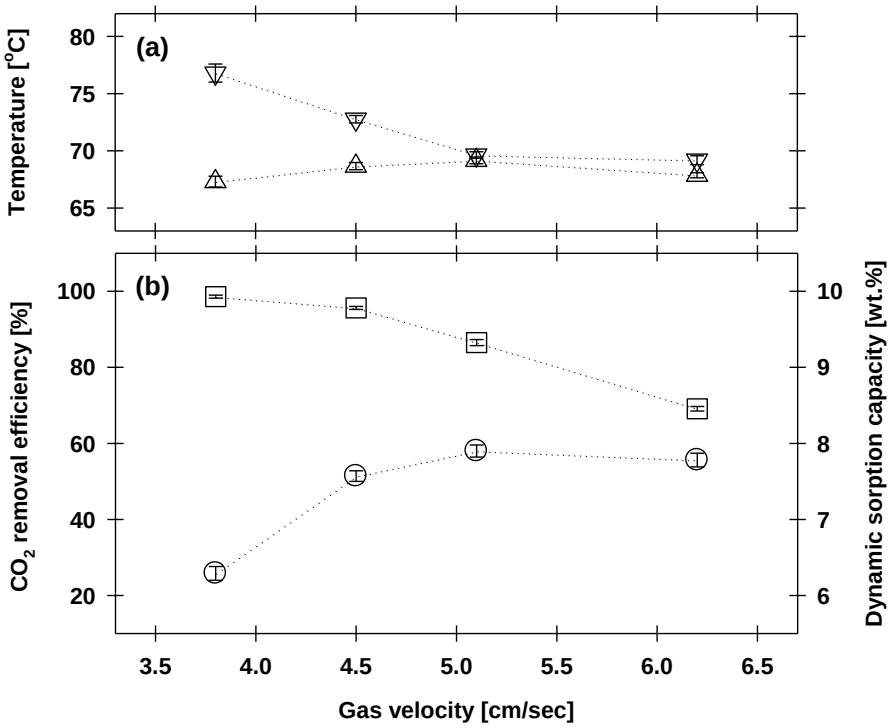
(a)
(b)
Temperature [°C]
CO2 removal efficiency [%]
Dynamic sorption capacity [wt.%]
Gas velocity [cm/sec]
80
75
70
65
100
80
60
40
20
10
9
8
7
6
3.5
4.0
4.5
5.0
5.5
6.0
6.5

Figure 3.

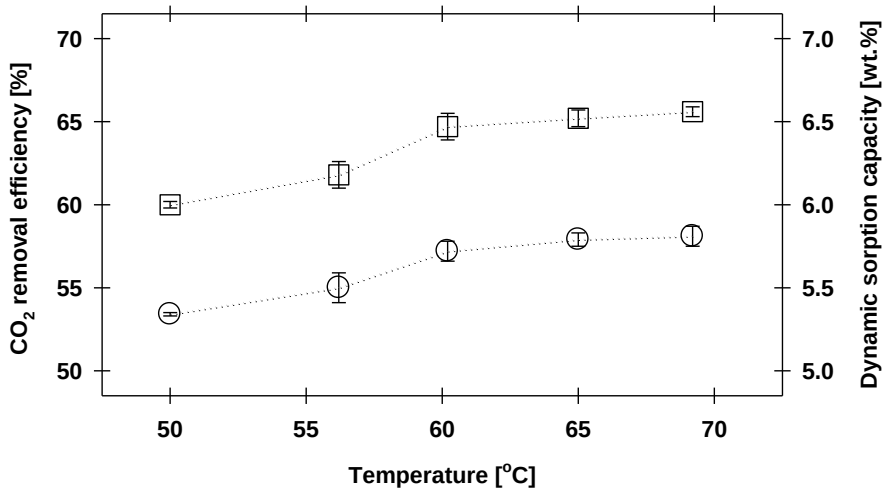
70
65
60
55
50
CO_2 removal efficiency [%]
7.0
6.5
6.0
5.5
5.0
Dynamic sorption capacity [wt.%]
50
55
60
65
70
Temperature [°C]

Figure 4.

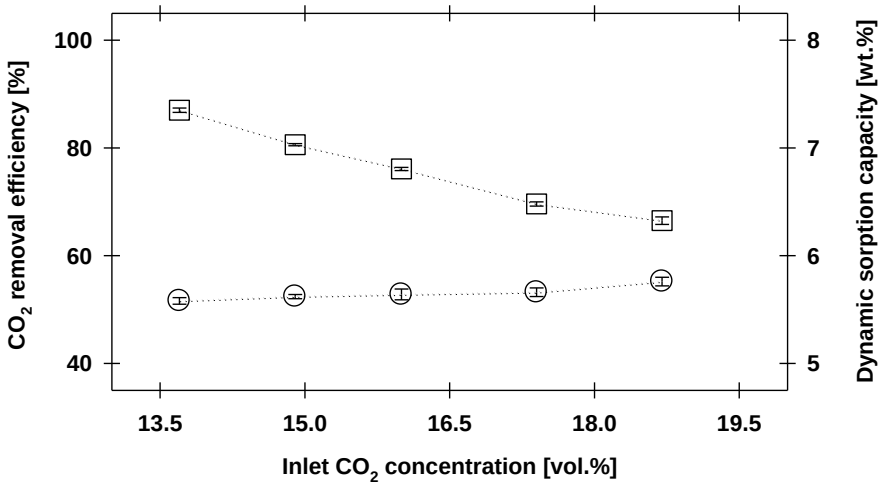
100
80
60
40
8
7
6
5
13.5
15.0
16.5
18.0
19.5
CO2 removal efficiency [%]
Dynamic sorption capacity [wt.%]
Inlet CO2 concentration [vol.%]

Figure 5.

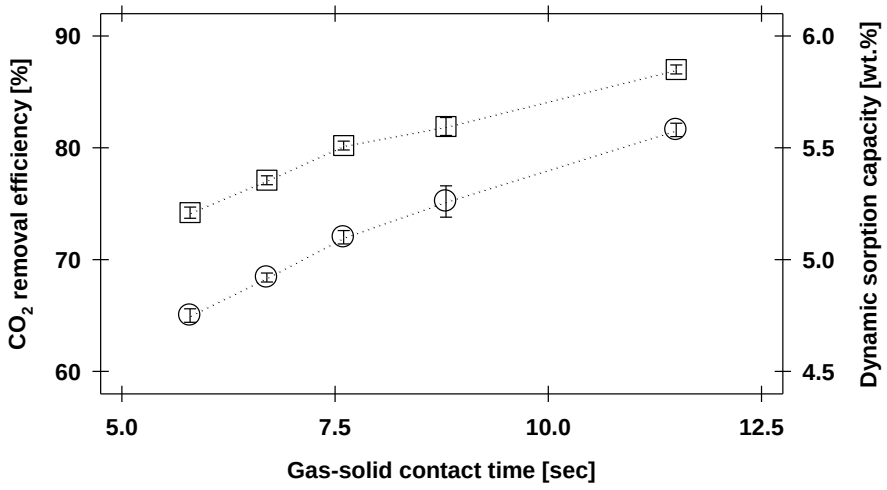
90
80
70
60
CO_2 removal efficiency [%]
6.0
5.5
5.0
4.5
Dynamic sorption capacity [wt.%]
5.0
7.5
10.0
12.5
Gas-solid contact time [sec]

Figure 6.

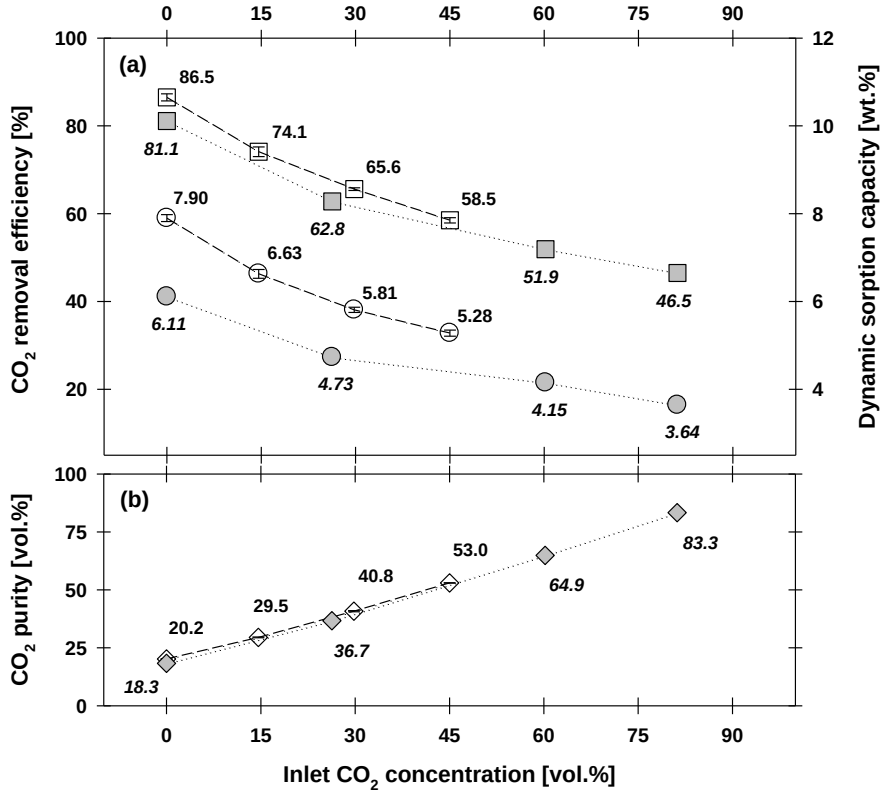
(a)
(b)
CO_2 removal efficiency [%]
Dynamic sorption capacity [wt.%]
CO_2 purity [vol.%]
Inlet CO_2 concentration [vol.%]
86.5
74.1
65.6
58.5
81.1
62.8
51.9
46.5
7.90
6.63
5.81
5.28
6.11
4.73
4.15
3.64
20.2
29.5
40.8
53.0
83.3
18.3
36.7
64.9

Figure 7.

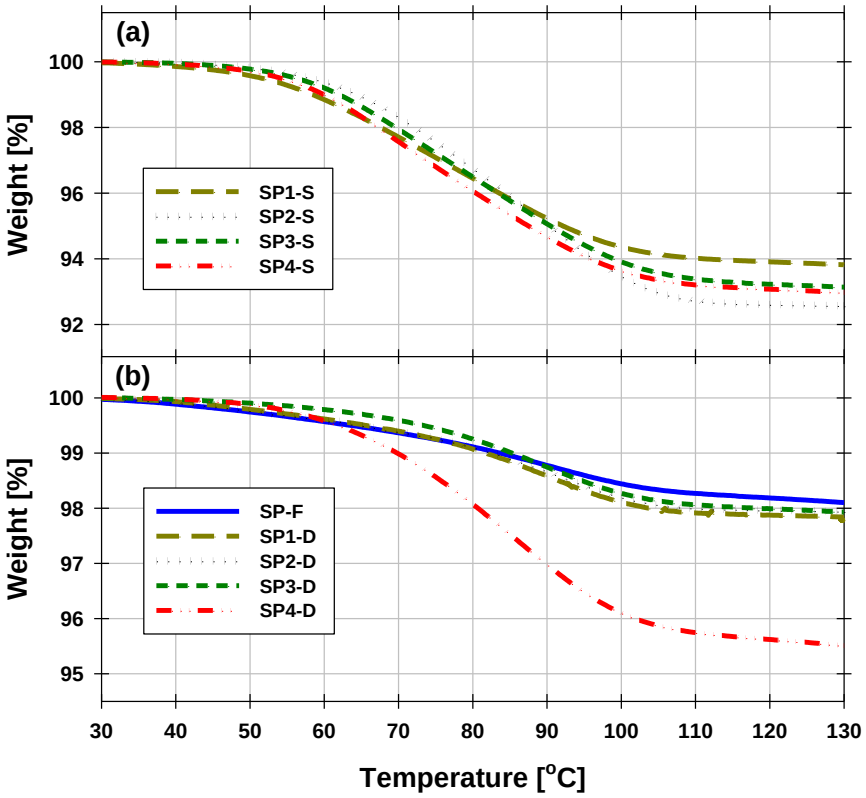
(a)
Weight [%]
100
98
96
94
92
SP1-S
SP2-S
SP3-S
SP4-S
(b)
Weight [%]
100
99
98
97
96
95
SP-F
SP1-D
SP2-D
SP3-D
SP4-D
30
40
50
60
70
80
90
100
110
120
130
Temperature [°C]

Figure 8.

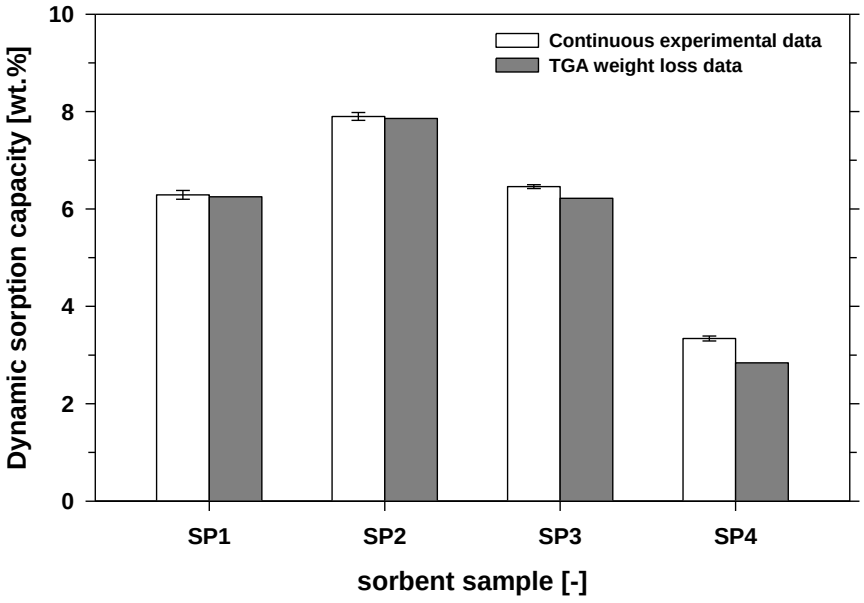
Continuous experimental data
TGA weight loss data
Dynamic sorption capacity [wt.%]
10
8
6
4
2
0
SP1
SP2
SP3
SP4
sorbent sample [-]

Figure 9.

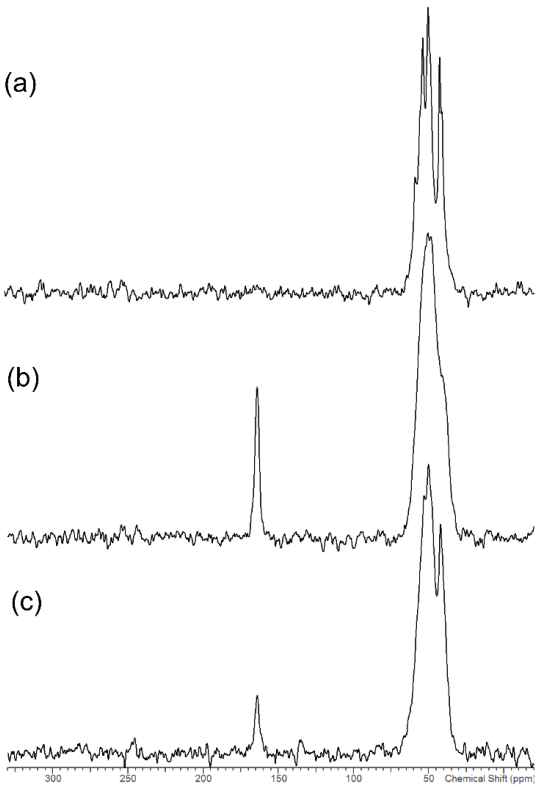

Figure 10.

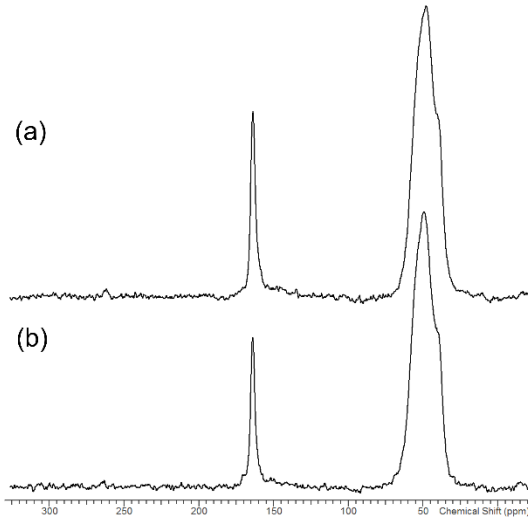

Figure 11.

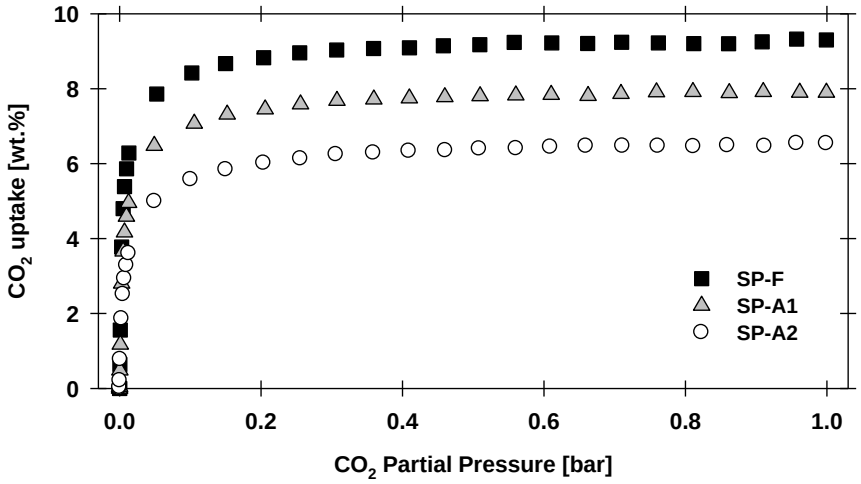
10
8
6
4
2
0
0.0
0.2
0.4
0.6
0.8
1.0
CO2 uptake [wt.%]
CO2 Partial Pressure [bar]
SP-F
SP-A1
SP-A2

Figure 12.